대한 유전성 대사 질환 : 2020;20(1):1~13

원 저

Glucosylceramide와 glucosylsphingosine에 의해 유도되는 신경세포 사멸에 대한 HDAC 저해제의 억제 효과 연구

이화여자대학교 의과대학 생화학교실

정남희 · 남유화 · 박세영 · 김지연 · 정성철

Inhibitory Action of a Histone Deacetylase 6 Inhibitor on Glucosylceramide- and Glucosylsphingosine-induced Neuronal Cell Apoptosis

Namhee Jung, Yu Hwa Nam, Saeyoung Park, Ji Yeon Kim, Sung-Chul Jung

Department of Biochemistry, College of Medicine,
Ewha Womans University, Seoul, Republic of Korea

Purpose: Gaucher disease (GD), which is the most prevalent lysosomal storage disorder worldwide, is caused by mutations in the glucocerebrosidase gene (GBA). GD is divided into three clinical subtypes based on the appearance of neurological symptoms. Type 1 GD is a chronic non-neuronopathic disease, and types 2 and 3 are acute neuronopathic and chronic neuronopathic forms, respectively. Neuronopathic GD types 2 and 3 are characterized by increased levels of glucosylceramide (GlcCer) and glucosylsphingosine (GlcSph) in the brain, leading to massive loss of neurons.

Methods: DNA damage and subsequent apoptosis of H4 cells were observed following neuroglioma H4 cell culture with GlcCer or GlcSph. Neuronal cell apoptosis was more prominent upon treatment with GlcSph.

Results: When H4 cells were treated with GlcSph in the presence of tubacin, a histone deacetylase 6 inhibitor (HDAC6i), attenuation of both DNA damage and a reduction in the protein expression levels of GlcSph-induced apoptosis-associated factors were observed.

Conclusion: These findings indicated that GlcSph played a prominent role in the pathogenesis of neuronopathic GD by inducing apoptosis, and that HDAC6i could be considered a therapeutic candidate for the treatment of neuronopathic GD.

Key words: Glucosylceramide, Glucosylsphingosine, Apoptosis, Gaucher disease, Neuronopathic, Histone deacetylase inhibitor

Introduction

Gaucher disease (GD) is an autosomal recessive lysosomal storage disorder that is caused by mutations in the *GBA1* gene encoding glucocerebrosidase (GCase)[1]. Deficiency in GCase activity leads to intracellular accumulation of its substrates (glucosylceramide and glucosylsphingosine). The patients with GD have classically been divided into three clinical subtypes, namely types 1, 2 and 3, which are distinguished by the absence

책임저자: 정성철, 서울특별시 강서구 마곡동로2길 25
이화여자대학교 의과대학 생화학교실
Tel: 02)6986-6199, Fax: 02)6986-7016
E-mail: jungsc@ewha.ac.kr

(type 1) or presence (types 2 and 3) of neuronopathic manifestations. In GD, common clinical symptoms include hepatosplenomegaly, pancytopenia, thrombocytopenia, and bone crisis. Types 2 and 3 neuronopathic GD are characterized by severe neuronophagia, astrocytosis and microglial nodule formation[2-6].

Although some therapeutic candidates, such as Ambroxol and venglustat, have been under clinical investigation for neuronopathic GD, there is no approved treatment available to date and little is known regarding the molecular mechanism leading to neurodegeneration. Abnormal folding of mutant GCase leads to the accumulation of this protein in the endoplasmic reticulum (ER). The accumulation and defective trafficking of mutant GCase from the ER to lysosomes can generate ER stress[7]. In addition, the loss of GCase activity results in diverse defects in the autophagy-lysosome system and in the mitochondrial function of GD subjects. Mitochondrial dysfunction causes reduced structural integrity, impaired activity of mitochondrial electron-transport chain and increased levels of reactive oxygen species. Prolonged ER stress and mitochondrial dysfunction result in the induction of apoptosis via the activation of caspases and the downregulation of Bcl-2[7-9]. Acute apoptosis has been observed in autopsy specimens from perinatal lethal GD, which is consistent with the aforementioned mechanism of action[10]. In a previous study, apoptotic neuronal cell death was detected in the brain tissues of a GD mouse model[9].

HDAC6 is a member of the histone deacetylase (HDAC) enzymes, which is involved in diverse biological processes, including regulation of cell structure and motility, induction of autophagy, regulation of immune processes, and the degradation of mis-folded proteins[11]. It has been reported that HDAC6 modulates the clearance of pathological protein aggregates or deposits in several neurological disorders. Trichostatin A (TSA), a selective inhibitor of HDAC6 (HDAC6i), may alleviate neuronal toxicity in Huntington's disease by increasing the acetylation of α-tubulin and subsequently increasing microtubule-based transport and promoting the activation of the degradation pathway[12]. In an Alzheimer disease model, TSA restored the decreased velocity and motility of the mitochondria in hippocampal neurons, and decreased concomitantly tau levels in the mouse brain tissues[13]. Although the detailed mechanism of action has not been fully investigated, in order to elucidate which HDAC inhibitor (HDACi) affects GCase stability, Yang et al[14], demonstrated that SAHA, a pan-HDACi, modulated the acetylation of Hsp90β and rescued GCase mutants from Hsp90β-mediated degradation in GD patients and fibroblast cell lines.

GD patients who experience neuropathy present with increased levels of glucosylsphingosine (GlcSph) that has frequently been characterized as a potential neurotoxic mediator. It is important to note that the development of other lysosomal sphingolipid diseases, such as Krabbe and Niemann-Pick diseases, has been attributed to the accumulation of the deacylated substrates responsible for neuronal cell loss and damage[15-17]. According to the study by Svennerholm et al[18], the deacylated form of glucosylceramide (GlcCer), namely GlcSph, was detected at extremely high concentrations in the brain tissues of patients with neuronopathic GD. These observations support the theory that the accumulation of GlcSph may contribute to the severity of neurological impairment in neuronopathic GD by activating the apoptotic cascade.

In the present study, we investigated the effects of GlcCer and GlcSph with regard to the

neuronopathic mechanism of GD. We examined whether the HDAC6i tubacin, was an effective therapeutic candidate for the suppression of apoptosis-induced signaling in neuronal cells.

Materials and Methods

1. Cell culture and sphingolipid treatment

The H4 human astrocytoma cell line (#HTB-148, ATCC, Manassas, VA, USA) was grown in Dulbecco's Modified Eagle Medium (DMEM, Invitrogen, Carlsbad, CA, USA) containing 10% fetal bovine serum (FBS, Invitrogen) according to the manufacturer's instructions. For sphingolipid treatment, H4 cells were seeded in triplicate in 24-well plates at a density of 3.5×10^4 cells/well; the cells were cultured in DMEM containing 4% FBS. GlcCer (#1522, Matreya, State College, PA, USA) and GlcSph (#43659, Sigma-Aldrich, St. Louis, MO, USA) (stock concentration 10 mM) were dissolved in chloroform/methanol (2:1 by volume) and further diluted in DMEM with 4% FBS. The HDAC6i tubacin (#SML0065, Sigma-Aldrich) was dissolved in 10% dimethyl sulfoxide (DMSO, #D2659, Sigma-Aldrich) and stored at -20℃. The working concentration for this compound was 20 μM.

2. Assessment of cell viability using an MTT assay

H4 cells were cultured in DMEM containing 4% FBS and 6 μM GlcCer or GlcSph. Following culture with GlcCer or GlcSph for 10 min, 30 min, 1, 5 and 20 h, respectively, MTT assays were performed. At each time point, the culture medium was removed and the MTT reagent (#M2128, thiazolyl blue tetrazolium bromide, Sigma-Aldrich) was added to the 24 well-plate. The cells were incubated at 37℃ for 2 h. The MTT reagent was subsequently removed and DMSO was added to each well to dissolve the formazan crystals. The absorbance of each well was measured at 560 nm with an ELISA reader (SynergyH1, BioTek, Winooski, VT, USA). H4 cells cultured with 4% FBS medium were used as the non-treated control group for all the experiments.

3. Western blot analysis

H4 cells were treated with combinations of sphingolipids and 20 μM tubacin for the following time points: 10 min, 1, 5, 15 and 20 h. The cells were washed with phosphate buffered saline (PBS), detached and incubated with PRO-PREP buffer (iNtRON Biotechnology, Seongnam-si, Korea) containing a phosphatase inhibitor cocktail solution (#P3200, GenDEPOT, Barker, TX, USA) on ice. The lysates were collected by centrifugation at 13,000×g for 20 min at 4℃ and equal amounts of protein from the supernatants were separated by SDS-PAGE. The resolved proteins were transferred onto polyvinylidene membranes (#P2938, Millipore, Burlington, MA, USA). The membranes were probed overnight at 4℃ with antibodies against the p-p38 mitogen-activated protein kinase (MAPK; 1:400, Cat no. 9216; Cell Signaling Technology, Danvers, MA, USA), p- Protein kinase B (AKT; Ser473; 1:300, Cat no. 9271; Cell Signaling Technology), AKT (1:300, Cat no. 9272; Cell Signaling Technology), cleaved Poly (ADP-ribose) polymerase (PARP; 1:500, Cat no. 9546; Cell Signaling Technology), caspase 3 (1:500, Cat no. 9662; Cell Signaling Technology), cytochrome c (1:500, Cat no. 4280; Cell Signaling Technology) and GAPDH (1:5,000, Cat no. LF-PA0212; Ab-Frontier, Seoul, Korea). The following morning,

incubation with the secondary antibody was performed. Goat anti-mouse IgG (1:2,500; cat. no. SC-2005; Santa Cruz Biotechnology, Inc., Dallas, Texas, USA) and goat anti-rabbit IgG (1:2500; cat. no. 7074; Cell Signaling Technology) were used as the secondary antibodies. The blots were washed and developed using enhanced chemiluminescence reagents SuperSignal West Dura (Cat no. 34076; Thermo Scientific, Waltham, MA, USA), according to the manufacturer's instructions. The images were captured with a densitometric scanning instrument (LAS-3000, Fujifilm, Tokyo, Japan).

4. Immunofluorescent detection of Ki67

The cells were fixed in 4% paraformaldehyde (15 min, room temperature) and washed three times in ice-cold PBS. For permeabilization, the cells were incubated in PBS containing 0.25% Triton X-100 for 10 min and rinsed in PBS three times. Following blocking with 1% bovine serum albumin (Bovogen Biologicals, Keilor East, VIC, Australia) for 1 h, the cells were incubated overnight at 4℃ with an anti-Ki67 antibody (1:200, Cat no. sc-15402; Santa Cruz Biotechnology, Inc.). Following rinsing in PBS, secondary goat anti-rabbit antibodies conjugated with Alexa Fluor 488 were applied for 1 h at room temperature in the dark. The cells were mounted and stained with Vectashield H-1200 containing DAPI (Cat no. H-1200; Vector Laboratories, Burlingame, CA, USA). The cells were observed with an Olympus BX51 phase-contrast microscope (Olympus, Tokyo, Japan).

5. TUNEL assay

A TUNEL assay was performed using an *in situ* death detection kit (Cat no. 11684795910; Sigma-Aldrich) according to the manufacturer's protocol. Briefly, the coverslips were fixed with paraformaldehyde and permeabilized with 0.1% Triton X-100 in 0.1% sodium citrate buffer. The fixed cells were incubated in reagent buffer (1:10 dilution of the enzyme solution in label solution) in a humidified chamber for 60 min at 37℃.

6. Statistical analysis

The results are presented as the mean±standard error of the mean. The data were analyzed by the two-way analysis of variance followed by Bonferroni's post hoc test. GraphPad Prism version 4 was used for statistical analysis of the results (GraphPad Software, Inc., San Diego, CA, USA). $P<0.05$ was considered to indicate a statistically significant difference. All the experiments were performed at least three times.

Results

1. GlcSph induces growth arrest in H4 cells

The effects of GlcCer or GlcSph on the brain-derived cell line H4 were observed following short-term (<1 h) and long-term treatment (>5 h). To avoid overgrowth of H4 cells, H4 cells were cultured in DMEM media containing only a limited amount of FBS (4%) and experiments were conducted within 24 h following treatments, because growth of H4 cells cultured with 10% FBS were too fast to observe the characterization of cellular responses to GlcCer or GlcSph. Following 6 μM GlcCer treatment, rapid morphological changes were noted, including cytoplasmic contraction, cell rounding, bipolar elongation, and formation of spindle-like cytoplasm (Fig. 1A). Following GlcSph

treatment, ~50% of the cells became spherical and 30% of the remaining cells underwent a rounding process after only 1 h of treatment (Fig. 1A). Moreover, when H4 cells were grown in the presence of GlcSph for 20 h, considerable numbers of rounded cells were observed that were either non-viable or detached from the bottom of the culture.

To investigate whether the morphological alterations could cause secondary effects, such as cell cycle arrest or decreased proliferation, MTT assays and Ki67 staining were used to analyze cells treated with GlcCer or GlcSph, respectively. At 20 h, GlcCer-treated cells indicated a decreased proliferative rate (1.8-fold) compared with that of the untreated group (2.3-fold). By contrast to GlcCer-treated cells, GlcSph treatment resulted in growth arrest and minimal cell death, as indicated by the reduced proliferative (1.5-fold) rate following 5 h of treatment (Fig. 1B). Nuclear staining analysis with the proliferation marker Ki67 indicated that the percentage of cells with a Ki67 positive stain was ~60.0% for GlcCer, whereas only 26.5% of cells were stained following treatment with GlcSph (Fig. 1C-1, 2).

2. H4 cell growth arrest by GlcSph treatment results in the induction of apoptosis

To determine the molecular mechanism of neurodegeneration in types 2 and 3 GD, the effects of GlcCer or GlcSph on the MAPK and AKT signaling pathways (which are associated with cell death and cell cycle arrest, respectively) were investigated.

Western blot analysis indicated that GlcCer caused a rapid increase in the levels of p38 MAPK phosphorylation. However, this effect was maintained for only 1 h. GlcSph exerted a delayed, but more prolonged response than GlcCer. The data

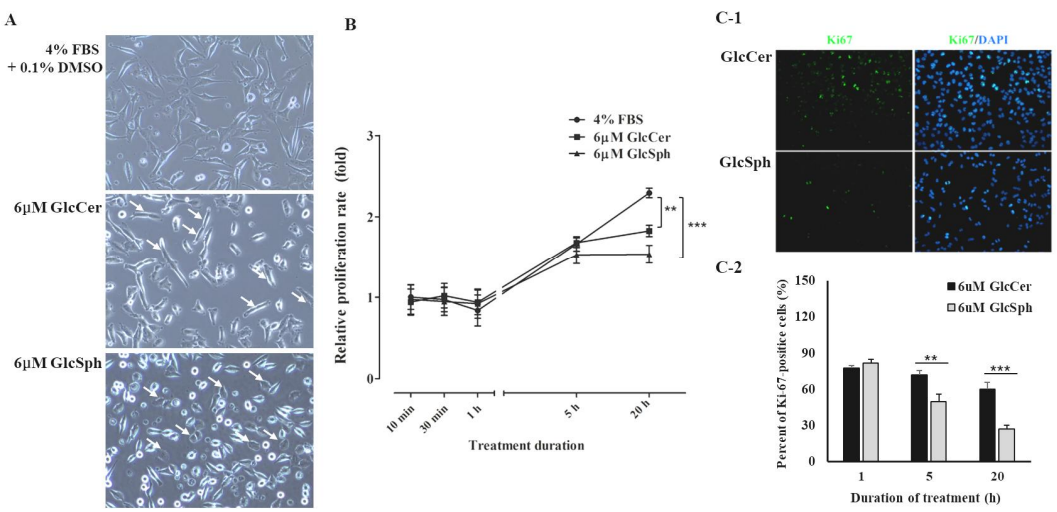

Fig. 1. GlcSph suppresses H4 cell growth. H4 Cells were treated with the indicated concentrations of GlcCer or GlcSph. (A) Rapid morphological changes of H4 cells by GlcCer or GlcSph were observed. Arrows indicate typical morphological changes observed in the fields (Fig. 1A). (B) Suppressed proliferation of H4 cells by GlcCer or GlcSph was observed based on MTT assays at 20 h. Proliferation rates were measured compared with the untreated control group as fold changes. (C-1) Following GlcCer or GlcSph treatment, the percentage of Ki67-positive proliferating cells was determined by immunocytochemistry at 20 h. The graph (C-2) shows a significant correlation between GlcSph treatment and the decrease in the number of Ki67-positive cells. Statistical analyses included two-way ANOVA followed by Bonferroni's post hoc test ($^{**}P<0.01$; $^{***}P<0.001$). GlcSph, glucosylsphingosine; GlcCer, glucosylceramide.

indicated that at the 5 h time point, phospho-p38MAPK (p-p38MAPK) levels were 2.5-fold that of the baseline levels. The overall expression levels of total AKT and phospho-AKT (p-AKT) were not significantly affected by GlcCer treatment. However, GlcSph led to a rapid decrease in the levels of p-AKT and caused a further increase in the total levels of AKT at time points higher the 1 h of treatment (Fig. 2A, B).

Analysis of the apoptotic markers revealed that only low levels of PARP cleavage were observed in the GlcCer treated cells, whereas caspase 3 was inactivated. In contrast to GlcCer, GlcSph caused dramatic upregulation of PARP cleavage (cl.PARP) and caspase 3 activation (cl.caspase 3), which was initiated 15 h following treatment (Fig. 2A, B). The results suggested that apoptotic neuronal cell death in GD was primarily caused by the GlcSph rather than the GlcCer substrate. Furthermore, the data demonstrated that this phenomenon was dependent on the p38 MAPK/AKT signaling pathway.

It is interesting to note that cytochrome c, the mitochondrial initiator of apoptosis and the upstream activating signal of caspase 3, exhibited a time-dependent upregulation by GlcCer and only a mild increase by GlcSph treatment (Fig. 2A, B). The data suggested that treatment of H4 cells with 6 μM GlcCer induced mitochondrial stress. However, this was not sufficient to cause the induction of H4 cell apoptosis. Moreover, the induction of apoptosis mediated by GlcSph was not dependent on the mitochondrial signaling pathway.

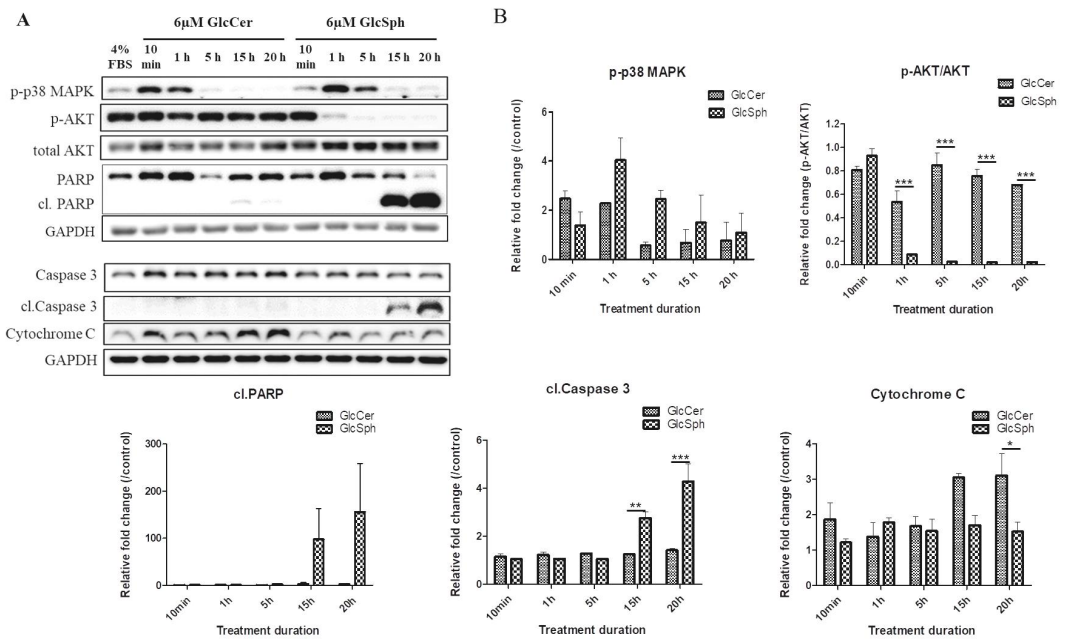

Fig. 2. Glucosylsphingosine-induced apoptotic cell death in the H4 cell line. (A) Western blot analysis of p-p38 MAPK, p-AKT, total AKT, PARP, cl.PARP (cleaved PARP), caspase 3, cl.caspase 3 (cleaved caspase 3) and cytochrome c are depicted. GAPDH was included as a loading control. (B) Bar graphs indicate the quantification of the p-p38 MAPK, p-AKT/total AKT, cl.PARP, cl.caspase 3 and cytochrome c proteins in the cells. The data were normalized according to the levels of GAPDH. Statistical analyses included two-way ANOVA followed by Bonferroni's post hoc test (*P<0.05; **P<0.01; ***P<0.001). GlcSph, glucosylsphingosine; p-, phosphorylated; MAPK, mitogen-activated protein kinase; AKT, Protein kinase B; PARP, Poly (ADP-ribose) polymerase; cl., cleaved.

3. The HDAC6i tubacin suppresses DNA damage induction by GlcSph

GlcSph exhibited nuclear condensation in the absence of cytosolic shrinkage (Fig. 1C-1). To investigate whether these abnormal responses were associated with DNA damage, TUNEL staining was conducted. Tubacin was applied for this analysis in order to assess the potential therapeutic effects caused by HDAC inhibition. The levels of TUNEL-positive cells were significantly increased in GlcSph-treated H4 cells following 20 h of treatment. In addition, following the combined application of tubacin and GlcSph, the TUNEL-positive cell ratio was decreased to approximately 31% of that of the tubacin-untreated group (Fig. 3).

4. The inhibition of AKT phosphorylation and the stimulation of p38 MAPK phosphorylation by GlcSph are suppressed by tubacin

To elucidate the molecular mechanism of tubacin-mediated-apoptosis, western blot analysis was performed. The data demonstrated that tubacin suppressed apoptosis-inducing signals by maintaining AKT phosphorylation and decreasing the levels of p38 MAPK phosphorylation. The rapid decrease in the levels of p-AKT expression that was caused in the first hour of GlcSph treatment was inhibited by tubacin treatment. In addition, the highest induction in the levels of the p-p38 MAPK expression (2.92-fold increase) noted at 1 h following GlcSph treatment was reduced to 1.59-fold (Fig. 4).

5. Tubacin induces structural changes in H4 cells

External treatment of H4 cells with GlcCer or GlcSph induced morphological changes. This rapid structural alteration was noted at the 1-h time point. Despite the diverse morphological changes caused by GlcCer treatment, GlcSph forced H4 cells to adopt only a rectangle shape. Following

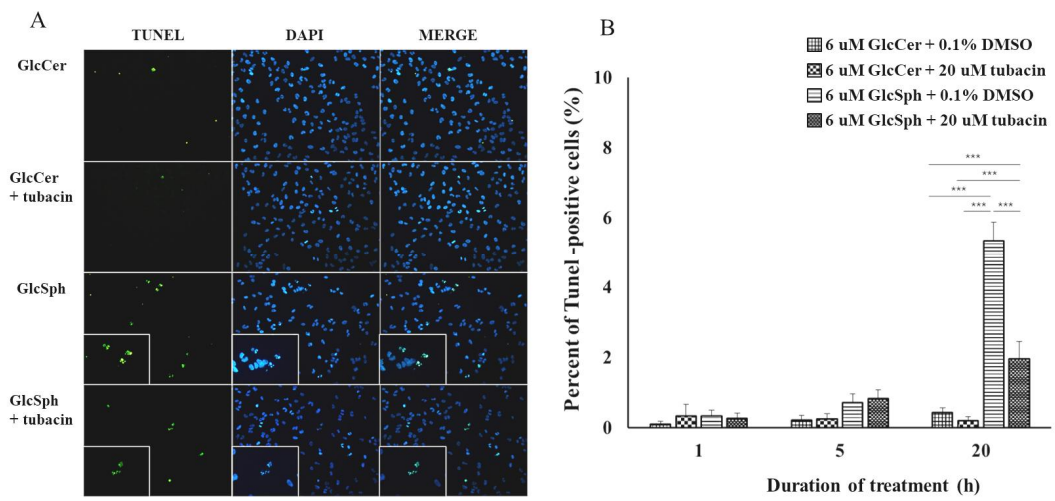

Fig. 3. HDAC6i reduces DNA damage induced by GlcSph treatment. (A) H4 cells were treated with GlcCer or GlcSph with or without HDAC6i (tubacin). The percentage of TUNEL-positive stained cells was determined by immunocytochemistry. The graph (B) shows significant correlation between tubacin treatment and the decrease of TUNEL-positive cells. Statistical analyses included two-way ANOVA followed by Bonferroni's post hoc test ($^{***}P<0.001$). HDAC6i, histone deacetylase 6 inhibitor; GlcSph, glucosylsphingosine; GlcCer, glucosylceramide.

5 h of incubation with GlcSph, ≥80% of the cells exhibited a round shape. However, treatment of the cells with tubacin reduced this morphological change. At the 1- and 5-h time points, the GlcSph- and tubacin-treated cells indicated additional attached edges than the cells treated solely with GlcSph (Fig. 5). Moreover, these cells underwent slower morphological changes. This result implied that tubacin may be involved not only in the suppression of the apoptotic mechanism but also in the maintenance of the cytoskeletal structure.

Discussion

The present study focused on the apoptotic effects of GlcSph that were associated with neuronopathic GD. Although there were not so much differences of morphological changes and decreased proliferation of H4 cells were observed treated with either GlcCer or GlcSph for 5 h, GlcSph treatment was more significantly affected to the cellular responses of H4 cells compared to GlcCer treatment for 20 h. The proliferation of H4 cells treated with GlcSph decreased to 65% of control value and expression of Ki67 also deceased to 73.5% of control value, while the proliferation of H4 cells treated with GlcCer decreased to 78% of control value and expression of Ki67 decreased to 60% of control value. The analysis of apoptotic markers indicated that apoptotic cell death of H4 cells was primarily caused by the GlcSph rather

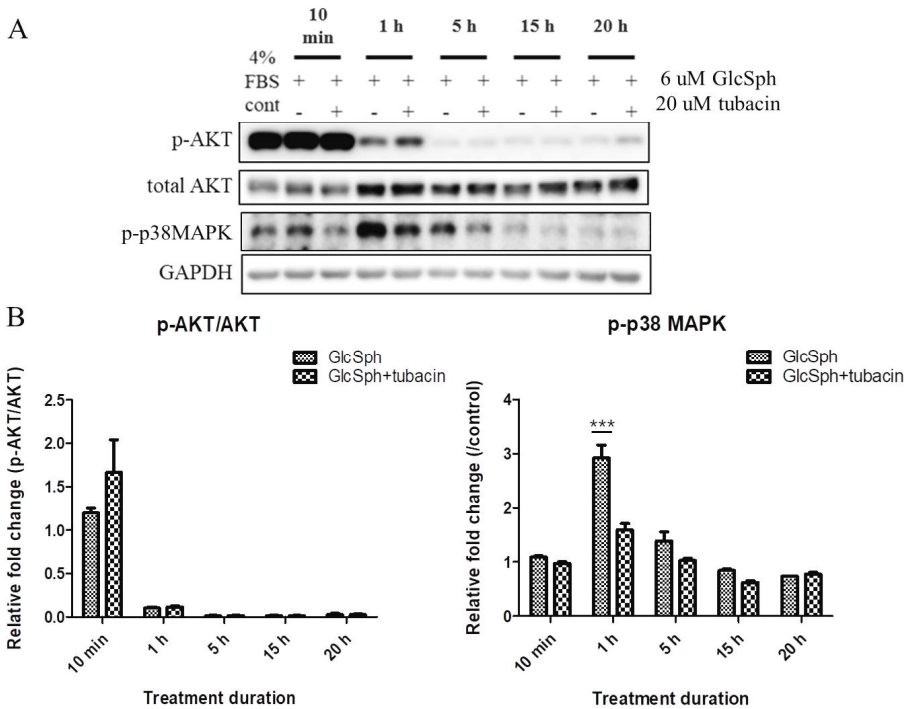

Fig. 4. Inhibition of AKT phosphorylation and stimulation of p38 MAPK phosphorylation by GlcSph are suppressed by tubacin. (A) Western blotting of p-AKT, total AKT, and p-p38 MAPK protein expression levels is depicted. (B) The bar graphs indicate the quantification of p-AKT/ total AKT, and p-p38 MAPK proteins in the cells. The data were normalized to GAPDH. Statistical analyses included two-way ANOVA followed by Bonferroni's post hoc test (***P<0.001). AKT, Protein kinase B; MAPK, mitogen- activated protein kinase; GlcSph, glucosylsphingosine; p-, phosphorylated.

than GlcCer and the p38 MAPK/AKT signaling pathways were involved in the H4 cell apoptosis. Non-neuronopathic type 1 GD is considered a preventable disease provided that national epidemiological monitoring can lead to early diagnosis and timely enzyme-replacement therapy[1,19-22]. However, in the case of neuronopathic GD (types 2 and 3), which involves central nervous system (CNS) pathology, no significant progress has been made with regard to the development of therapeutic approaches. Furthermore, the underlying mechanisms involved in neuronal cell death are not fully understood. Since diverse tools have been developed for the accurate monitoring of GlcCer and GlcSph levels in patients, it has been proposed that GlcSph is not only a sensitive biomarker for type 1 GD but also a main determinant of clinical severity[23-25]. Recent data support the conclusion that GlcSph is suitable as a prospective marker for neuronopathic GD as well as type 1 GD, since its levels are more specifically upregulated compared with the levels of GlcCer in the brain tissues of GD patients and GD mice[18,26]. Moreover, Tylki-Szymanska et al[27], demonstrated that GlcSph levels correlated with chitotriosidase activity, which is a GD biomarker. The results were derived from 64 GD patient plasma samples. In this cohort study, the authors highlighted that following ERT treatment, both GlcSph levels and chitotriosidase activity were downregulated. This effect correlated with the dose of ERT[27]. GlcCer and GlcSph are direct storage substrates that are metabolized by GCase. However, the maximum rate of enzymatic hydrolysis for GlcSph is clearly lower than that noted for GlcCer. Moreover, GlcSph exhibits water-soluble features. Therefore, it is likely that GlcSph may play a role as a systemic and neurological toxic agent[28].

To determine the mechanisms associated with the neuronopathic phenotype, various cell and animal models can be applied. These models can be genetically modified, chemically induced or exogenously treated with sphingolipids[29-33]. Despite their widespread use, they exhibit several

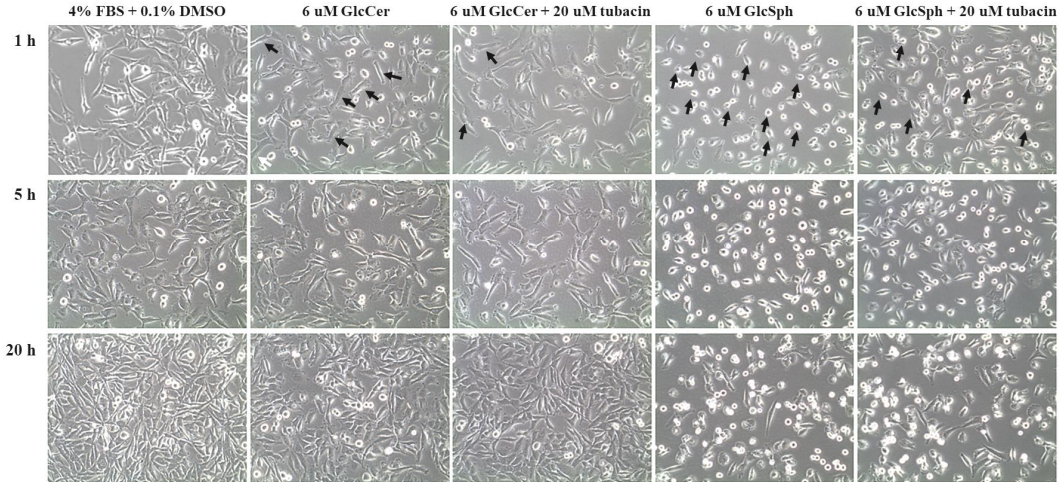

Fig. 5. GlcSph-mediated growth inhibition is ameliorated by tubacin treatment. Representative microscopy images captured with an Olympus phase-contrast microscope IX51 (Olympus) showing the effect on cells that were treated with GlcCer or GlcSph with or without tubacin. (A-a-c); 4% FBS+0.1% DMSO (B-a-c); 6 μM GlcCer (C-a-c); 6 μM GlcCer+20 μM tubacin, (D-a-c); 6 μM GlcSph and (E-a-c); 6 μM GlcCer+20μM tubacin for 1, 5 and 20 h (magnification, ×200). Arrows indicate typical morphological changes observed in the fields. GlcSph, glucosylsphingosine; GlcCer, glucosylceramide.

limitations, such as the adjustment of disease severity and the different ratio of increased GlcCer or GlcSph levels among the same mutation type [32]. Recent studies by Vitner et al[34], concluded that the neuronal cell death noted in neuronopathic GD was mainly induced by the Rip kinase pathway, and that it was directly involved in several pathological events. Global gene expression profiling was performed using skin fibroblast cells from GD patients to understand the pathological mechanisms of GD[35]. This research group analyzed the molecular changes in GD subjects by comparing them with those from other lysosomal storage disorders, Niemann-Pick disease and normal healthy control subjects. In this study, the authors confirmed that the expression levels of the immune response genes were significantly altered in GD subjects. These genes were involved in the Jak-Stat, type II interferon, interferon gamma, and PI3K-AKT signaling pathways[35]. A previous study demonstrated that the expression levels of the mature forms of all 3 cathepsins (cathepsin B, K, and S) were increased in the spleen and plasma samples of GD subjects. The pathological functions of cathepsins in GD were categorized into induction of tissue destruction, abnormal immune regulation, and defective osteoclast activity[36]. Further studies using various neuronal cells from GD animal models or patients and other neuronal cell types besides H4 cells should be needed to clarify neuronopathic mechanisms in GD, because only apoptotic cell death of H4 cells was analyzed in this present study.

Although early studies on HDACi were focused on their role as suppressors of tumor cell growth, recent studies have demonstrated that they can lead to neuronal cell survival in a diverse range of neurodegenerative diseases[37-39]. Notably, the clinical application of HDACi for the treatment of GCase mutated-associated diseases, such as Alzheimer's disease and Parkinson's disease have been reported[40,41]. With regard to GD, a previous case has been reported that investigated the therapeutic mechanism of HDACi using GD patient-derived fibroblasts[42]. According to that study, the misfolded GCase was degraded via the valosin-containing protein (VCP)-associated pathway, and during that process, HDACi could suppress GCase degradation by maintaining the levels of acetylated HSP90β, which is the chaperone modulator of VCP [14,42]. Hyperacetylated HSP90β resulted in limited degradation of abnormal GCase, and therefore, the expression levels and the activity of GCase were retained. While the previous studies focused on the maintenance of innate GCase protein stability, the present study demonstrated the effects of HDACi on the suppression of neuronal cell death induced by external treatment of glycosphingolipids. A cell model was used in order to demonstrate the inhibition of GlcSph-specific cell damage and apoptotic activation following HDACi treatment.

The HDAC6i tubacin suppressed GlcSph-stimulated apoptosis via DNA damage prevention, dephosphorylation of p38 MAPK, and retention of AKT phosphorylation. A previous study has shown increased levels of p-p38 MAPK in the lung and liver tissues of the GD mouse model[43]. Furthermore, among the three types of GD mouse models, only the neuronopathic GD model indicated significant activation of the p38 MAPK in brain tissues. These data suggested that p38 MAPK was involved in GD pathology and that it may also be a reliable target for therapeutic purposes. In the present study, p38 MAPK was examined and revealed to be activated by both exogenous GlcCer and GlcSph treatment. However, the activation of p38 caused by GlcSph exhibited a higher duration and magnitude. Therefore, we tested whether

HDACi could suppress the GlcSph-induced abnormal p38 MAPK phosphorylation. Surprisingly, p38 MAPK phosphorylation was decreased by tubacin at various time points. Moreover, the maximum levels of expression of phosphorylated p38 at 1 h were reduced to approximately half of the baseline levels. Tubacin further contributed to the apoptosis-resistance phenotype by preventing DNA damage and inducing AKT phosphorylation, which was consistent with previous studies[44,45].

The present study demonstrated that tubacin, a specific HDAC6i, exhibited therapeutic potency on neuronal cell death in a GD cell model. Moreover, the data indicated that the survival mechanisms induced by tubacin were associated with GlcSph-mediated early apoptotic signaling. Unfortunately, these observations were restricted to confirming the potential of this compound to suppress early apoptosis-related signaling and did not address the reduction in the apoptotic death population. To examine the possible use of tubacin as a therapeutic agent for neuronopathic GD, further studies are required to elucidate the processes by which HDAC6i promotes cell survival.

요 약

Gaucher disease (GD)는 glucocerebrosidase 유전자(GBA)의 돌연변이에 의하여 발병하는 전세계적으로 가장 유병율이 높은 리소좀 축적질환이다. GD는 신경학적인 증상의 유무에 따라 3가지 임상형으로 구분된다. 신경병증 GD인 2형과 3형의 경우는 대뇌에서 glucosylceramide (GlcCer)와 glucosylsphingosine (GlcSph)의 농도가 증가하면서 신경세포의 심각한 손실이 야기되는 특징을 보인다.

신경교종에서 유래한 H4 세포를 GD에서 증가하는 기질인 GluCer와 GlcSph를 첨가하여 배양하였을 때, 심각한 DNA손상과 더불어 세포의 사멸이 야기되는 것과 이러한 신경세포의 사멸은 GluCer 보다는 GlcSph을 처리하였을 때 더 현저하게 증가하는 것을 관찰하였다. H4 세포에 히스톤 탈아세틸화 효소(HDAC) 6의 저해제인 tubacin과 GlcSph을 함께 처리하였을 경우에는 DNA손상은 물론 GlcSph에 의하여 유도된 세포사멸과 관련된 단백질 인자들의 발현이 모두 감소되었다. 본 연구를 통해 GlcSph이 세포사멸을 통하여 신경병증 GD의 발병에 주요한 역할을 한다는 것을 알 수 있었고, HDAC6 저해제가 신경병증 GD 환자를 위한 치료제 후보물질로 제시될 수 있는 가능성을 확인하였다.

References

1) Grabowski GA. Phenotype, diagnosis, and treatment of Gaucher's disease. Lancet 2008;372:1263-71.
2) Vellodi A. Lysosomal storage disorders. Brit J Haematol 2005;128:413-31.
3) Kaplan P, Andersson HC, Kacena KA, Yee JD. The clinical and demographic characteristics of nonneuronopathic Gaucher disease in 887 children at diagnosis. Arch Pediatr Adolesc Med 2006;160:603-8.
4) Langeveld M, Elstein D, Szer J, Hollak CEM, Zimran A. Classifying the additional morbidities of Gaucher disease. Blood Cells Mol Dis 2018;68:209-10.
5) Conradi NG, Sourander P, Nilsson O, Svennerholm L, Erikson A. Neuropathology of the Norrbottnian type of Gaucher disease. Morphological and biochemical studies. Acta Neuropathol 1984;65:99-109.
6) Farfel-Becker T, Vitner EB, Pressey SN, Eilam R, Cooper JD, Futerman AH. Spatial and temporal correlation between neuron loss and neuroinflammation in a mouse model of neuronopathic Gaucher disease. Hum Mol Genet 2011;20:1375-86.
7) Shen HM, Mizushima N. At the end of the autophagic road: An emerging understanding of lysosomal functions in autophagy. Trends Biochem Sci 2014;39:61-71.
8) Wei H, Kim SJ, Zhang Z, Tsai PC, Wisniewski KE, Mukherjee AB. ER and oxidative stresses are common mediators of apoptosis in both neurodegenerative and non-neurodegenerative lysosomal storage disorders and are alleviated by chemical chaperones. Hum Mol Genet 2008;17:469-77.
9) Hong YB, Kim EY, Jung SC. Down-regulation of Bcl-2 in the fetal brain of the Gaucher disease mouse model: A possible role in the neuronal loss. J Hum

Genet 2004;49:349-54.
10) Finn LS, Zhang M, Chen SH, Scott CR. Severe type II Gaucher disease with ichthyosis, arthrogryposis and neuronal apoptosis: Molecular and pathological analyses. Am J Med Genet 2000;91:222-6.
11) Liu KP, Zhou D, Ouyang DY, Xu LH, Wang Y, Wang LX, et al. LC3B-II deacetylation by histone deacetylase 6 is involved in serum-starvation-induced autophagic degradation. Biochem Biophys Res Commun 2013;441:970-5.
12) Iwata A, Riley BE, Johnston JA, Kopito RR. HDAC6 and microtubules are required for autophagic degradation of aggregated huntingtin. J Biol Chem 2005;280:40282-92.
13) Kim C, Choi H, Jung ES, Lee W, Oh S, Jeon NL, et al. HDAC6 inhibitor blocks amyloid beta-induced impairment of mitochondrial transport in hippocampal neurons. PLoS One 2012;7:e42983.
14) Yang C, Rahimpour S, Lu J, Pacak K, Ikejiri B, Brady RO, et al. Histone deacetylase inhibitors increase glucocerebrosidase activity in Gaucher disease by modulation of molecular chaperones. Proc Natl Acad Sci U S A 2013;110:966-71.
15) Chuang WL, Pacheco J, Zhang XK, Martin MM, Biski CK, Keutzer JM, et al. Determination of psychosine concentration in dried blood spots from newborns that were identified via newborn screening to be at risk for Krabbe disease. Clin Chim Acta 2013;419:73-6.
16) Chuang WL, Pacheco J, Cooper S, McGovern MM, Cox GF, Keutzer J, et al. Lyso-sphingomyelin is elevated in dried blood spots of Niemann-Pick B patients. Mol Genet Metab 2014;111:209-11.
17) Gelb MH, Scott CR, Turecek F. Newborn screening for lysosomal storage diseases. Clin Chem 2015;61:335-46.
18) Nilsson O, Svennerholm L. Accumulation of glucosylceramide and glucosylsphingosine (psychosine) in cerebrum and cerebellum in infantile and juvenile Gaucher disease. J Neurochem 1982;39:709-18.
19) Stirnemann J, Vigan M, Hamroun D, Heraoui D, Rossi-Semerano L, Berger MG, et al. The French Gaucher's disease registry: Clinical characteristics, complications and treatment of 562 patients. Orphanet J Rare Dis 2012;7:77.
20) Berger J, Stirnemann J, Bourgne C, Pereira B, Pigeon P, Heraoui D, et al. The uptake of recombinant glucocerebrosidases by blood monocytes from type 1 Gaucher disease patients is variable. Br J Haematol 2012;157:274-7.
21) Yoshida S, Kido J, Matsumoto S, Momosaki K, Mitsubuchi H, Shimazu T, et al. Prenatal diagnosis of Gaucher disease using next-generation sequencing. Pediatr Int 2016;58:946-9.
22) Vigan M, Stirnemann J, Caillaud C, Froissart R, Boutten A, Fantin B, et al. Modeling changes in biomarkers in Gaucher disease patients receiving enzyme replacement therapy using a pathophysiological model. Orphanet J Rare Dis 2014;9:95.
23) Fuller M, Szer J, Stark S, Fletcher JM. Rapid, single-phase extraction of glucosylsphingosine from plasma: A universal screening and monitoring tool. Clin Chim Acta 2015;450:6-10.
24) Dekker N, van Dussen L, Hollak CE, Overkleeft H, Scheij S, Ghauharali K, et al. Elevated plasma glucosylsphingosine in Gaucher disease: Relation to phenotype, storage cell markers, and therapeutic response. Blood 2011;118:e118-27.
25) Rolfs A, Giese AK, Grittner U, Mascher D, Elstein D, Zimran A, et al. Glucosylsphingosine is a highly sensitive and specific biomarker for primary diagnostic and follow-up monitoring in Gaucher disease in a non-Jewish, Caucasian cohort of Gaucher disease patients. PLoS One 2013;8:e79732.
26) Hamler R, Brignol N, Clark SW, Morrison S, Dungan LB, Chang HH, et al. Glucosylceramide and glucosylsphingosine quantitation by liquid chromatography-tandem mass spectrometry to enable in vivo preclinical studies of neuronopathic Gaucher disease. Anal Chem 2017;89:8288-95.
27) Tylki-Szymanska A, Szymanska-Rozek P, Hasinski P, Lugowska A. Plasma chitotriosidase activity versus plasma glucosylsphingosine in wide spectrum of Gaucher disease phenotypes - A statistical insight. Mol Genet Metab 2018;123:495-500.
28) Vaccaro AM, Muscillo M, Suzuki K. Characterization of human glucosylsphingosine glucosyl hydrolase and comparison with glucosylceramidase. Eur J Biochem 1985;146:315-21.
29) Westbroek W, Nguyen M, Siebert M, Lindstrom T, Burnett RA, Aflaki E, et al. A new glucocerebrosidase-deficient neuronal cell model provides a tool to probe pathophysiology and therapeutics for Gaucher disease. Dis Model Mech 2016;9:769-78.
30) Hein LK, Meikle PJ, Hopwood JJ, Fuller M. Secondary sphingolipid accumulation in a macrophage model of Gaucher disease. Mol Genet Metab 2007;92:336-45.
31) Schueler UH, Kolter T, Kaneski CR, Blusztajn JK, Herkenham M, Sandhoff K, et al. Toxicity of glucosylsphingosine (glucopsychosine) to cultured neuronal cells: A model system for assessing neuronal damage in Gaucher disease type 2 and 3. Neurobiol Dis 2003;14:595-601.
32) Farfel-Becker T, Vitner EB, Futerman AH. Animal

models for Gaucher disease research. Dis Model Mech 2011;4:746-52.
33) Enquist IB, Lo Bianco C, Ooka A, Nilsson E, Månsson JE, Ehinger M, et al. Murine models of acute neuronopathic Gaucher disease. Proc Natl Acad Sci U S A 2007;104:17483-8.
34) Vitner EB, Salomon R, Farfel-Becker T, Meshcheriakova A, Ali M, Klein AD, et al. RIPK3 as a potential therapeutic target for Gaucher's disease. Nat Med 2014;20:204-8.
35) Lugowska A, Hetmanczyk-Sawicka K, Iwanicka-Nowicka R, Fogtman A, Ciesla J, Purzycka-Olewiecka JK, et al. Gene expression profile in patients with Gaucher disease indicates activation of inflammatory processes. Sci Rep 2019;9:6060.
36) Moran MT, Schofield JP, Hayman AR, Shi GP, Young E, Cox TM. Pathologic gene expression in Gaucher disease: up-regulation of cysteine proteinases including osteoclastic cathepsin K. Blood 2000;96:1969-78.
37) Johnstone RW. Histone-deacetylase inhibitors: Novel drugs for the treatment of cancer. Nat Rev Drug Discov 2002;1:287-99.
38) Wang Y, Wang X, Liu L, Wang X. Hdac inhibitor trichostatin A-inhibited survival of dopaminergic neuronal cells. Neurosci Lett 2009;467:212-6.
39) Kim SJ, Lee BH, Lee YS, Kang KS. Defective cholesterol traffic and neuronal differentiation in neural stem cells of Niemann-Pick type C disease improved by valproic acid, a histone deacetylase inhibitor. Biochem Biophys Res Commun 2007;360:593-9.
40) Seo J, Jo SA, Hwang S, Byun CJ, Lee HJ, Cho DH, et al. Trichostatin A epigenetically increases calpastatin expression and inhibits calpain activity and calcium-induced SH-SY5Y neuronal cell toxicity. FEBS J 2013;280:6691-701.
41) Barkhuizen M, Anderson DG, Grobler AF. Advances in GBA-associated Parkinson's disease-Pathology, presentation and therapies. Neurochem Int 2016;93:6-25.
42) Lu J, Yang C, Chen M, Ye DY, Lonser RR, Brady RO, et al. Histone deacetylase inhibitors prevent the degradation and restore the activity of glucocerebrosidase in Gaucher disease. Proc Natl Acad Sci U S A 2011;108:21200-5.
43) Kitatani K, Wada M, Perry D, Usui T, Sun Y, Obeid LM, et al. Activation of p38 Mitogen-Activated Protein Kinase in Gaucher's Disease. PLoS One 2015;10:e0136633.
44) Khan S, Jena G. Sodium butyrate, a Hdac inhibitor ameliorates eNOS, iNOS and TGF-beta1-induced fibrogenesis, apoptosis and DNA damage in the kidney of juvenile diabetic rats. Food Chem Toxicol 2014;73:127-39.
45) Kaliszczak M, Trousil S, Ali T, Aboagye EO. AKT activation controls cell survival in response to HDAC6 inhibition. Cell Death Dis 2016;7:e2286.